Dynamics of dissociative adsorption of hydrogen on a CO-precovered Ru(0001) surface: A comparison of theoretical and experimental results

Irene M. N. Groot[1,2],* Juan Carlos Juanes-Marcos[1], Cristina Díaz[1,3], Mark F. Somers[1], Roar A. Olsen[1,4], and Geert-Jan Kroes[1]

[1]*Leiden Institute of Chemistry, Leiden University, P.O. Box 9502, 2300 RA Leiden, The Netherlands*

[2]*FOM Institute for Plasma Physics Rijnhuizen, P.O. Box 1207, 3430 BE Nieuwegein, The Netherlands*

[3]*Departamento de Química C-9, Universidad Autónoma de Madrid, 28049 Madrid, Spain and*

[4]*Akershus University College, P.O. Box 423, N-2001 Lillestrøm, Norway*

(Dated: October 15, 2009)

Supplementary information

Modified Shepard interpolation method

In the modified Shepard (MS) interpolation method, the interpolated PES is given by a weighted series of second order Taylor expansions centered on DFT data points, sampled throughout the configuration space of the system. Instead of the interatomic distances R_i, the inverse interatomic distances, $Q_i = 1/R_i$, are used to describe the PES, which gives a better mathematical behavior (the singularities at $R_i \rightarrow 0$, when any two atoms are close to each other, are transformed away to $Q_i \rightarrow \infty$). The vector defining any configuration of the system is given by $\mathbf{Q} = [1/R_1, ..., 1/R_{n(n-1)/2}]$, where n is the number of atoms used to describe the system. We modeled the CO/Ru(0001) by using the symmetry unique area of the $(\sqrt{3}\text{x}\sqrt{3})R30^\circ$ surface unit cell, *i.e.* the equilateral triangle in Fig. S1, which is half of the $(\sqrt{3}\text{x}\sqrt{3})R30^\circ$ unit cell. Six atoms were used to describe the H_2 + CO/Ru(0001) interaction: The two hydrogen atoms of the H_2 molecule approaching the surface, and four surface atoms (three O atoms at the corners of the equilateral triangle, and a Ru atom at the center, see Fig. S1). We have also tested other representations of the surface, but they gave either worse results (*e.g.* if the Ru atom at the center of the triangle is not taken into account), or similar results while consuming much more CPU time (*e.g.* if also the three C atoms located below the O atoms are considered).

In our case, $n = 6$, so we have $n(n-1)/2 = 15$ interatomic distances. However, the PES is a function of only $3n - 6 = 12$ independent internal coordinates (eliminating the six translational and rotational degrees of freedom). For each system configuration, the $3n - 6$ internal coordinates, ζ, are defined as linear combinations of the inverse interatomic distances $\mathbf{Q}$[1]:

$$\zeta_m = \sum_{k=1}^{n(n-1)/2} U_{mk} Q_k \qquad (m = 1, ..., 3n-6). \tag{1}$$

Note that different configurations $\mathbf{Q}$ of the system will have different transformation matrices $\mathbf{U}$, and therefore different definitions of the (local) internal coordinates ζ[1]. The potential energy at any configuration $\mathbf{Q}$, near data point $\mathbf{Q}(i)$, can be expanded as a second-order Taylor expansion $T_i(\mathbf{Q})$:

$$T_i(\mathbf{Q}) = V[\mathbf{Q}(i)] + \sum_{k=1}^{3n-6} [\zeta_k - \zeta_k(i)] \frac{\partial V}{\partial \zeta_k}\bigg|_{\mathbf{Q}=\mathbf{Q}(i)}$$
$$+ \frac{1}{2} \sum_{k=1}^{3n-6} \sum_{j=1}^{3n-6} [\zeta_k - \zeta_k(i)][\zeta_j - \zeta_j(i)] \frac{\partial^2 V}{\partial \zeta_k \delta \zeta_j}\bigg|_{\mathbf{Q}=\mathbf{Q}(i)} + ... \quad (2)$$

Here $V[\mathbf{Q}(i)]$, the value of the potential energy at data point $\mathbf{Q}$(i), and the gradients with respect to ζ at this point were calculated analytically with DFT. The second derivatives of the potential were calculated using numerical forward finite differences of the gradients.

The interpolated potential energy at any configuration Q is then given by

$$V(\mathbf{Q}) = \sum_{g \in G} \sum_{i=1}^{N_{data}} w_{g \circ i}(\mathbf{Q}) T_{g \circ i}(\mathbf{Q}), \quad (3)$$

where $T_{g \circ i}(\mathbf{Q})$ represents a second-order Taylor expansion, and $w_{g \circ i}(\mathbf{Q})$ a normalized weight function (for more details see Refs. 1 and 2). N_{data} is the number of DFT data points in the interpolation, G is the symmetry group of the system and $g \circ i$ is the transformation of the ith data point by the group element g. To take into account the symmetry of the system, a sum is performed over both the DFT data points and all their symmetry equivalent points. In the MS interpolation method the sampling of DFT data points is not uniformly distributed over the configuration space, which presents an advantage over other interpolation methods, which require a regular grid of data points (see *e.g.* Refs. 3 and 4). In the dynamically important regions of the PES, a larger number of data points is computed. These regions are found by performing classical trajectory calculations. The philosophy behind this method is that it is only necessary to know the PES in that region of space where the dynamics takes place. New points were chosen and added to the PES data set according to one of the following criteria[1,5,6]: (i) The h-weight criterium, where it is assumed that the new point should be added in the region which is most frequently visited by the classical trajectories, unless (too) many data points are already present there, and (ii) the variance criterium, where it is assumed that a new point should be added in the region where the extrapolation of the Taylor expansion is the most inaccurate.

'Growth' of the PES data set

The PES data set was 'grown' according to the following iterative scheme[1,5,6]:

(i) We started with an initial PES data set, which contained 105 data points located along six different reaction paths. Those reaction paths were found from DFT results obtained from 2D (r,Z) cuts through the full 6D PES, and by (adaptive) nudged elastic band calculations (see Ref. 7 for further details).
(ii) Using this initial PES 10 classical trajectories were run on the interpolated PES.
(iii) From the configurations visited by these classical trajectories a new point was chosen and added to the PES data set according to one of the above described criteria.
(iv) After updating the PES data set by adding the new point, the grow process was continued at the second step.
(v) After ~ 200 new points were added to the PES, its accuracy was checked by computing the reaction and scattering probabilities from a classical trajectory simulation using 5000 trajectories per set of initial conditions. If the reaction probability was not converged (*i.e.* if the reaction probability curve differed from the one computed in the previous simulation based on a smaller potential data base), we returned to the second step and continued the process. Otherwise, when convergence was achieved, the grow process was stopped.

To ensure an accurate representation of the PES over the whole energy range possibly probed by a molecular beam for hydrogen molecules, we grew the PES simultaneously at several kinetic energies and rovibrational quantum states (see Table S1). In the grow process we only considered H_2 molecules colliding at normal incidence. To obtain an accurate PES for H_2 + CO/Ru(0001) the grow process had to continue until 3495 extra data points in addition to the 105 initial points were added to the PES data set. The location of the PES data points (both the initial and the added ones) is shown in Fig. S2, in (X, Y) and (r, Z) 2D subspaces. We note that Fig. S2a shows the actually calculated data points, as well as their symmetry equivalent ones, obtained by rotating 120° and 240° around the three-fold axis (see Fig. S1). Fig. S3 shows the results of the convergence of the reaction probability for kinetic energies of 0.3 and 0.8 eV, and for a few selected initial states.

Quasi-classical trajectory calculations

To find the dynamically important regions of the PES during the grow process and to calculate reaction probabilities, we performed quasi-classical trajectory (QCT) calculations[8]. The initial zero point energy (ZPE) of the hydrogen molecule was included in the dynam-

ics by using an ensemble of initial conditions for the internal motion of the molecules that forms a classical microcanonical distribution. QCT calculations are susceptible to the so-called ZPE violation problem[9]. However, for an activated process such as H_2 dissociation on CO/Ru(0001), this problem is expected to play only a minor role at energies above the threshold to reaction, and the QCT method is known to give accurate results for activated molecule-surface reactions[10–16]. In contrast to the fully classical method, vibrational softening (adiabatic transfer of energy from internal to translational motion) is taken into account in an approximate way, whereas not doing this may lead to underestimated reaction probabilities for activated dissociation[13]. As noted below, we perform a quantum dynamics calculation for one initial rovibrational state to validate the use of the quasi-classical trajectory method[15].

To compute the reaction probability of hydrogen we integrated the classical equations of motion using the velocity-Verlet algorithm[17]. For each initial kinetic energy (E_{kin}) and initial rovibrational state (v, J, m_J), the probabilities have been calculated as an average over the molecular initial conditions, *i.e.* internal coordinates and internal momenta conjugate to these coordinates. To obtain the molecular initial conditions for each set of initial parameters E_{kin}, v, J and m_J, a Monte Carlo sampling method has been used. In order to minimize the statistical errors we have computed 5000 trajectories for each value of E_{kin} and rovibrational state (v, J, m_J) of H_2 (D_2). This leads to a maximum error in the reaction probabilities reported of 0.007. We have used an integration time step of 0.01 a.u. (*i.e.* 2.4×10^{-4} fs) and a total propagation time of 5000 a.u (*i.e.* 121 fs). The allowed error in the energy conservation of each trajectory has been set to 10^{-3} a.u. (*i.e.* 27 meV). We consider that dissociation has taken place whenever $r > 4a_0$ (2.1 Å) with a positive radial velocity of H_2. In contrast, a molecule is considered reflected when the molecular center-of-mass Z reached its starting point with the molecule's velocity vector pointing towards the vacuum.

To compute reaction probabilities as a function of m_J the initial angular momentum of the molecule was fixed according to $|\mathbf{L}| = \sqrt{J(J+1)}$. The orientation of $\mathbf{L}$ was chosen randomly with the constraint:

$$cos(\theta_L) = \frac{m_J}{\sqrt{J(J+1)}}, \tag{4}$$

where θ_L is the angle between $\mathbf{L}$ and the Z-axis (the axis perpendicular to the surface).

Quantum dynamics calculations

Quantum dynamics calculations have been performed by solving the time-dependent Schrödinger equation using the time-dependent wave packet (TDWP) method[18] in an implementation described in Ref. 13.

The initial state of the system [$\Psi(t = 0; \mathbf{r}, \mathbf{R})$, where $\mathbf{r} = (r, \theta, \varphi$ and $\mathbf{R} = (X, Y, Z)]$ is represented by the product of a Gaussian wave packet in Z and the rovibrational eigenfunctions of H_2 (v, J, m_J). For normal incidence

$$\Psi(t = 0; \mathbf{r}, \mathbf{R}) = N\varphi_{vJ}(r)Y_{Jm_J}(\theta, \varphi)e^{-\alpha(Z-Z_0)^2+ik_{av}Z}, \tag{5}$$

where the vibrational eigenfunction $\varphi_{vJ}(r)$ and the spherical harmonic $Y_{Jm_J}(\theta, \varphi)$ together describe the initial rovibrational state of the hydrogen molecule, N is a factor normalizing the wave packet, α is the width of the wave packet in Z and k_{av} is the average translational momentum of H_2 towards the surface.

To represent the dependence of the wave function on Z, r, X and Y, a direct product discrete variable representation (DVR)[19] with constant grid spacings $\Delta Z, \Delta r, \Delta X$ and ΔY is used. Fast Fourier transforms[20,21] are used to transform the wave function from coordinate to momentum space, and vice versa. To represent the dependence of the wave function on θ and φ, a non-direct product finite basis representation (FBR) of spherical harmonics $Y_{Jm_J}(\theta, \varphi)$ is used. Gauss-Legendre and Fourier transformations are used to transform the wave function from the non-direct product FBR to a direct product DVR in θ and φ[22,23], respectively, and vice versa.

To propagate the wave packet in time the split operator method[20] is used. The part of the wave packet that is reflected from the surface is analyzed[24], integrated over time and the S-matrix elements for all open rotation, vibration and diffraction channels are obtained. State-to-state scattering probabilities are computed from the S-matrix elements. All these scattering probabilities are summed over final states and subtracted from unity to obtain the initial-state-selected reaction probability. For more details we refer the reader to Refs. 15 and 25.

The parameters used in the calculations are described below. The values are given in Table S2 for the two different wave packets used, one for low kinetic energy (0.1-0.35 eV)

and one for high kinetic energy (0.3-0.8 eV). The initial wave packet was defined by the initial position of the center of the wave packet (Z_0) and its average initial momentum (k_{av}). The calculation is done on the Z grid, which is defined by its minimum value in Z, Z_i, the spacing ΔZ, and the number of grid points N_Z. To speed up the calculation, a projection operator approach[26] is used, in which the initial wave packet is moved towards the surface on a two-dimensional grid in Z and r, that is longer in Z than the 6D grid. This 2D grid is called the specular grid, and its number of points in the Z direction is given by N_Z^{sp}. The grid in r is defined in the same way as the grid in Z. The grid in X and Y is a periodic grid with a periodicity defined by the lattice constant and the number of grid points N_X and N_Y. The basis set in θ and φ is given by the maximum J value, J_{max}.

The reflected wave packet was analyzed at Z_∞, which is far enough from the surface to ensure that there is no interaction between the molecule and the surface. The wave packet is propagated in time with a time step Δt. We added an optical potential[27] to the Z and r grid to absorb the reflected (reacted) part of the wave packet before it reached the end of the grid. The optical potential is characterized by its start value, the range over which it extends and the value for the translational energy (here called the optical energy) for which the optimum absorption takes place[27].

---

* Electronic address: groot@chem.leidenuniv.nl

1 K. C. Thompson, M. J. T. Jordan, and M. A. Collins, *J. Chem. Phys.*, 1998, **108**, 8302.

2 C. Crespos, M. A. Collins, E. Pijper, and G. J. Kroes, *J. Chem. Phys.*, 2004, **120**, 2392.

3 H. F. Busnengo, A. Salin, and W. Dong, *J. Chem. Phys.*, 2000, **112**, 7641.

4 R. A. Olsen, H. F. Busnengo, A. Salin, M. F. Somers, G. J. Kroes, and E. J. Baerends, *J. Chem. Phys.*, 2002, **116**, 3841.

5 M. J. T. Jordan, K. C. Thompson, and M. A. Collins, *J. Chem. Phys.*, 1995, **102**, 5647.

6 R. P. A. Bettens and M. A. Collins, *J. Chem. Phys.*, 1999, **111**, 816.

7 I. M. N. Groot, J. C. Juanes-Marcos, R. A. Olsen, and G. J. Kroes, *J. Chem. Phys.*, submitted.

8 M. Karplus, R. N. Porter, and R. D. Sharma, *J. Chem. Phys.*, 1965, **43**, 3259.

9 Y. Guo, D. L. Thompson, and T. D. Sewell, *J. Chem. Phys.*, 1996, **104**, 576.

10 D. A. McCormack and G. J. Kroes, *Phys. Chem. Chem. Phys.*, 1999, **1**, 1359.

[11] G. J. Kroes, *Prog. Surf. Sci.*, 1999, **60**, 1.

[12] D. A. McCormack, G. J. Kroes, R. A. Olsen, I. A. Groeneveld, J. N. P. van Stralen, E. J. Baerends, and R. C. Mowrey, *Faraday Discuss.*, 2000, **117**, 109.

[13] E. Pijper, M. F. Somers, G. J. Kroes, R. A. Olsen, E. J. Baerends, H. F. Busnengo, A. Salin, and D. Lemoine, *Chem. Phys. Lett*, 2001, **347**, 277.

[14] P. Riviere, H. F. Busnengo, and F. Martín, *J. Chem. Phys.*, 2005, **123**, 074705.

[15] G. J. Kroes and M. F. Somers, *J. Theor. Comput. Chem.*, 2005, **4**, 493.

[16] C. Díaz, J. K. Vincent, G. P. Krishnamohan, R. A. Olsen, G. J. Kroes, K. Honkala, and J. K. Nørskov, *Phys. Rev. Lett.*, 2006, **96**, 096102.

[17] W. C. Swope, H. C. Andersen, P. H. Berens, and K. R. Wilson, *J. Chem. Phys.*, 1982, **76**, 637.

[18] R. Kosloff, *J. Phys. Chem.*, 1988, **92**, 2087.

[19] J. C. Light, I. P. Hamilton, and J. V. Lill, *J. Chem. Phys.*, 1985, **82**, 1400.

[20] M. D. Feit, J. A. Fleck, and A. Steiger, *J. Comput. Phys.*, 1982, **47**, 412.

[21] D. Kosloff and R. Kosloff, *J. Comput. Phys.*, 1983, **52**, 35.

[22] G. C. Corey and D. Lemoine, *J. Chem. Phys.*, 1992, **97**, 4115.

[23] D. Lemoine, *J. Chem. Phys.*, 1994, **101**, 10526.

[24] G. G. Balint-Kurti, R. N. Dixon, and C. C. Marston, *J. Chem. Soc., Faraday Trans.*, 1990, **86**, 1741.

[25] E. Pijper, G. J. Kroes, R. A. Olsen, and E. J. Baerends, *J. Chem. Phys.*, 2002, **117**, 5885.

[26] D. Neuhauser and M. Baer, *J. Chem. Phys.*, 1989, **91**, 4651.

[27] A. Vibok and G. G. Balint-Kurti, *J. Phys. Chem.*, 1992, **96**, 8712.

TABLE CAPTIONS

TABLE S1. Kinetic energies and rovibrational states (v, J, m_J) for which the PES data set was 'grown'.

TABLE S2. Parameters used in the TDWP calculations. All values are in atomic units, unless stated otherwise. See text for details.

FIGURE CAPTIONS

FIG. S1. Symmetry unique area of the CO/Ru(0001)-($\sqrt{3}$x$\sqrt{3}$)$R30°$ unit cell, where the PES is built by applying the MS interpolation method. The white circles represent CO molecules adsorbed perpendicularly to the surface. The black circles represent the Ru atoms in the first (top) layer (three Ru atoms are below the CO molecules). Four atoms are used to represent the surface in our model: the three O atoms at the corners of the triangle, and the Ru atom at its center. There is a threefold rotational axis passing through the centered Ru atom, and perpendicular to the surface.

FIG. S2. The initial data points of the PES data set (grey) and those added by the grow algorithm (black) shown in (X, Y) representation (top panel) and in (r, Z) representation (bottom panel).

FIG. S3. Convergence of the H_2 reaction probability with respect to the number of data points in the PES versus the reaction probability for kinetic energies of 0.3 eV (top panel) and 0.8 eV (bottom panel).

TABLE S1: Kinetic energies and rovibrational states (v, J, m_J) for which the PES data set was 'grown'.

Kinetic energy / eV	v	J	m_J
0.3	0	0	0
0.3	0	3	3
0.3	1	1	0
0.3	1	1	1
0.5	0	0	0
0.5	0	3	0
0.5	0	3	1
0.5	0	3	2
0.5	0	3	3
0.8	0	0	0
0.8	0	3	0
0.8	0	3	3

TABLE S2: Parameters used in the TDWP calculations. All values are in atomic units, unless stated otherwise. See text for details.

	Energy range (eV)	
Parameter	0.1-0.35	0.3-0.8
Initial wave packet		
Initial position Z_0	18.5	18.0
Average initial momentum k_{av}	7.46	12.21
Grid parameters		
Z_i	1.49	1.49
N_Z	128	128
N_Z^{sp}	256	256
Grid spacing ΔZ	0.15	0.15
r_i	0.4	0.4
N_r	32	32
Grid spacing Δr	0.25	0.25
N_X (N_Y)	32	48
Lattice constant	8.98	8.98
J_{max} rotational basis	18	18
Time propagation		
Time step Δt	2.5	2.5
Propagation time	120000	60000
Z optical potential		
Start optical potential	15.9	16.4
Optical energy	3.7×10^{-4}	3.7×10^{-4}
Range	3.15	3.65
r optical potential		
Start optical potential	4.15	4.15
Optical energy	3.7×10^{-3}	3.7×10^{-3}
Range	4.0	4.0
Other parameters		
Analysis value Z_∞	15.7	15.7

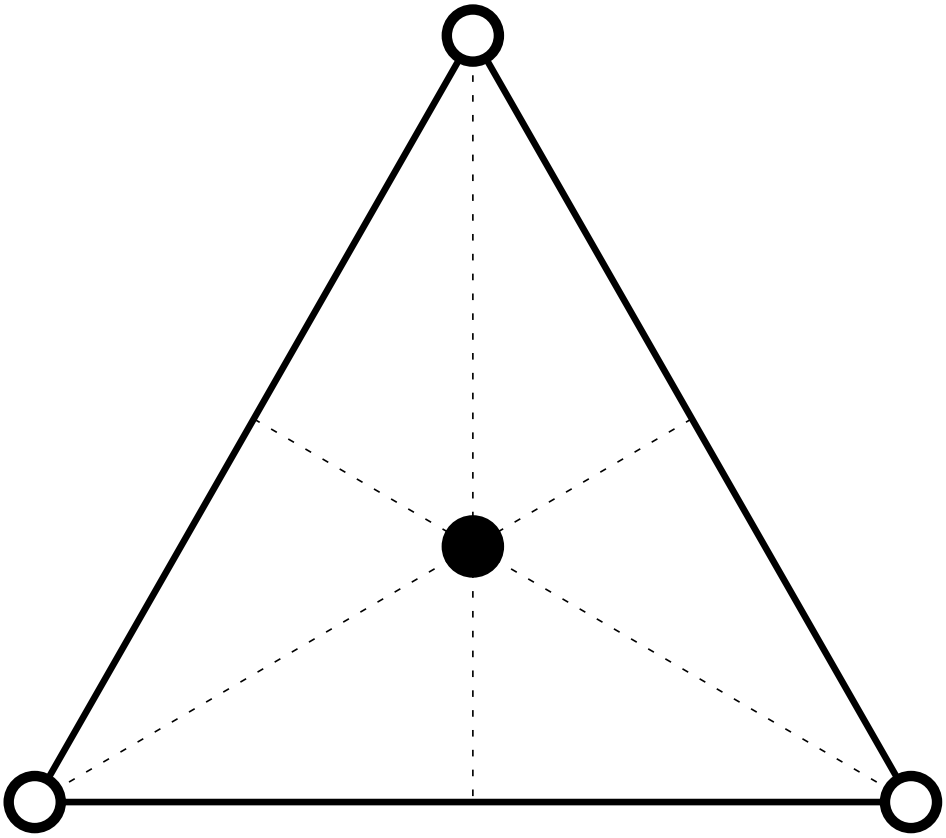

FIG. S1: Symmetry unique area of the CO/Ru(0001)-($\sqrt{3}$x$\sqrt{3}$)$R30°$ unit cell, where the PES is built by applying the MS interpolation method. The white circles represent CO molecules adsorbed perpendicularly to the surface. The black circles represent the Ru atoms in the first (top) layer (three Ru atoms are below the CO molecules). Four atoms are used to represent the surface in our model: the three O atoms at the corners of the triangle, and the Ru atom at its center. There is a threefold rotational axis passing through the centered Ru atom, and perpendicular to the surface.

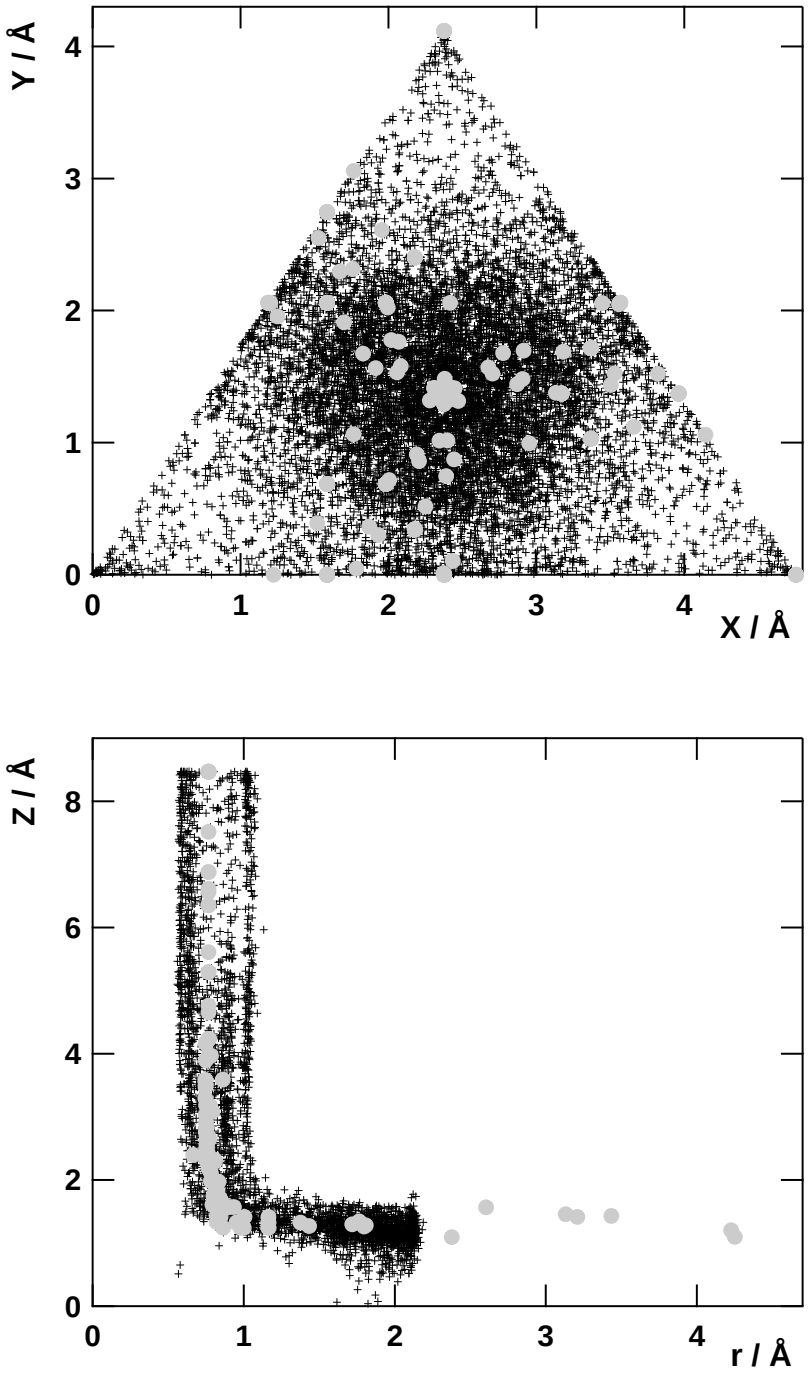

FIG. S2: The initial data points of the PES data set (grey) and those added by the grow algorithm (black) shown in (X, Y) representation (top panel) and in (r, Z) representation (bottom panel).

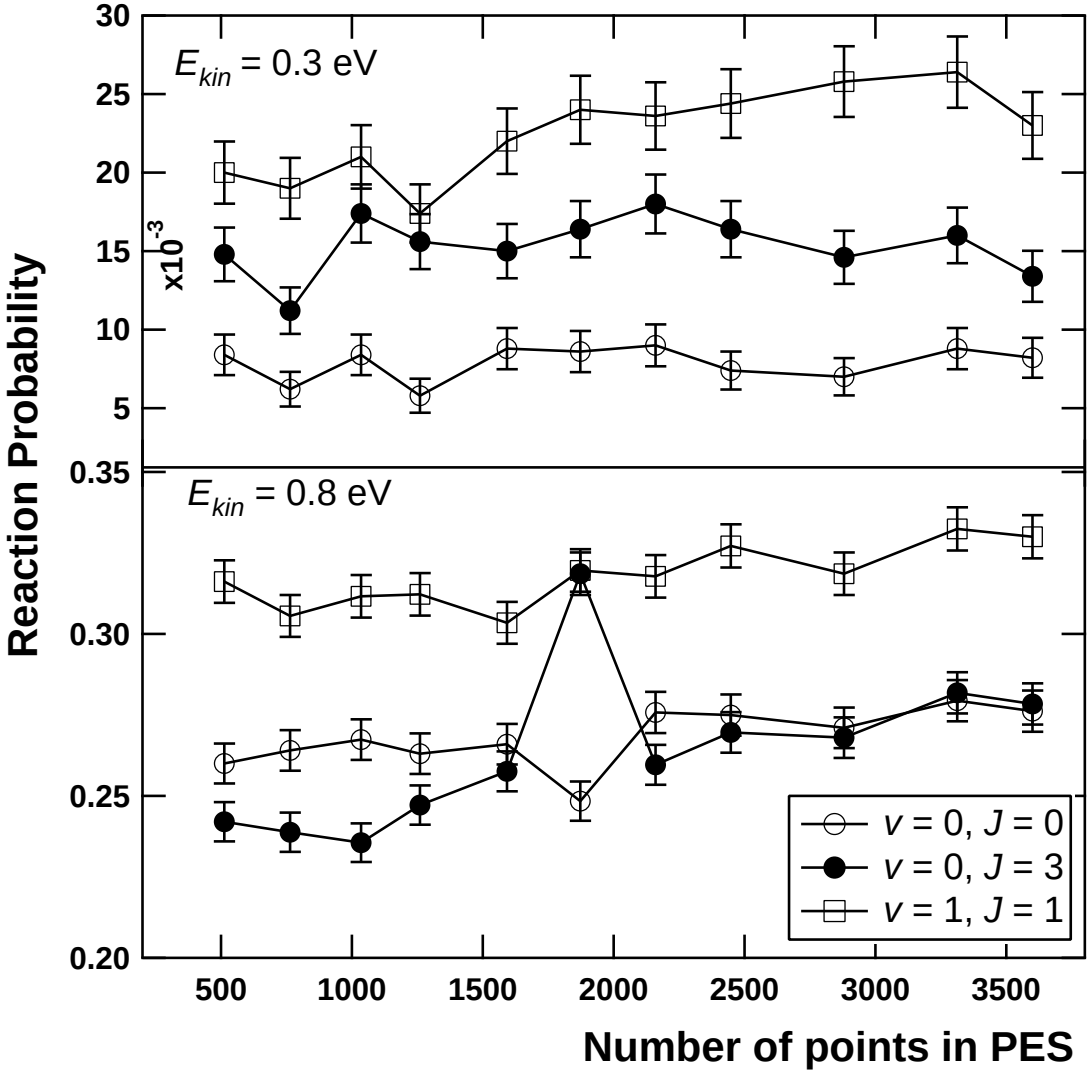

FIG. S3: Convergence of the H_2 reaction probability with respect to the number of data points in the PES versus the reaction probability for kinetic energies of 0.3 eV (top panel) and 0.8 eV (bottom panel).